Transition between Atomic and Molecular Hydrogen in the Galaxy: Vertical Variation of the Molecular Fraction

Kouitiro Imamura and Yoshiaki Sofue
Institute of Astronomy, University of Tokyo, Mitaka, Tokyo 181, Japan

Abstract

We derive radial and vertical distributions of HI and H_2 gas densities in our Galaxy by using the terminal velocity method. We calculate the molecular fraction ($f_{\rm mol}$) defined as the ratio of the molecular hydrogen to total hydrogen gas density at galactic longitude $l = 33^\circ \sim 64^\circ$ and galactic latitude $b = -2^\circ \sim +2^\circ$. The thickness of the molecular dominant region ($f_{\rm mol} \geq 0.8$) is approximately constant (109 ± 12 pc) at galactocentric distance $R \simeq$4.7$-$7.2 kpc. The molecular fraction decreases suddenly at a critical height from the galactic plane, below which the gas disk is almost totally molecular, while it is almost atomic beyond this height. We show that the vertical $f_{\rm mol}$ variation can be reproduced by a model which takes into account the phase transition between HI and H_2 gases in the interstellar matter.

Key Words: Atomic Hydrogen — the Galaxy — Interstellar Matter — Molecular Hydrogen

1 Introduction

The major constituents of the interstellar matter (ISM) in the Galaxy are the neutral atomic (HI) and molecular (H_2) hydrogen gases. The distributions of the HI and H_2 gases have been obtained through observations of the 21-cm and CO-line emissions, respectively. It is known that the HI gas is distributed in the outer region of the Galaxy, while H_2 gas is more concentrated toward the galactic center (e.g., Burton 1988; Combes 1991). However, the mutual relation of the distributions of HI and H_2 gases in the Galaxy, which will be deeply coupled with the transition between these two phases of the ISM, has been not yet investigated in detail.

Elmegreen (1993) has proposed a phase-transition theory of the HI and H_2 gases, in which the molecular fraction ($f_{\rm mol}$), as defined by the ratio of the H_2 gas mass density to the total hydrogen gas density, is determined by the interstellar pressure, UV radiation intensity and the metal abundance. Sofue *et al.* (1995) and Honma *et al.* (1995) have studied the radial variation of $f_{\rm mol}$ in several galaxies, and found that the molecular fraction decreases suddenly at a certain galactocentric distance, which they called the molecular front. They further modeled the molecular front phenomenon based on the phase-transition theory of the HI and H_2 gases in the ISM.

Since the Milky Way Galaxy has been observed extensively both in the HI and CO lines at much higher linear resolution than external galaxies, we may be able to study the molecular front phenomenon in the Galaxy not only in the radial direction but also in the perpendicular direction to the galactic plane. In this paper we analyze latitude-velocity ($b-v$) diagrams of the HI- and CO-line emissions of the Galaxy by applying the terminal velocity method, and derive the HI and H_2 gas distributions in the (R, z) plane, where R is the galactocentric distance and z is the height from the galactic plane. We further derive the distribution of the molecular fraction in the (R, z) plane, and investigate the hydrogen phase transition in the z direction. We also model the result based on the phase-transition theory of ISM.

2 Data and Procedure

2.1 Data

We use the HI survey of Bania and Lockman (1984) observed with the Arecibo 304-m radio telescope. The HI data are in the forming $b-v$ diagrams, and maps are sampled at intervals of $\Delta b = 2'$ with a half-power beamwidth of $4'$, and the latitude coverage is $\pm 3^\circ$. We also use the CO survey of Knapp *et al.* (1985) observed with the 7-m telescope at the Bell-Telephone Laboratories. The CO maps are sampled at intervals of $\Delta b = 2'$ with a half-power beamwidth of $100''$, and the latitude coverage is $\simeq \pm 2^\circ$. The longitude coverage of the HI and CO data are $l = 33^\circ \sim 64^\circ$ and $l = 10^\circ \sim 77^\circ$, respectively. Both maps are spaced at equal intervals in longitude: $\Delta \sin l = 0.025$. We used the Arecibo

HI data, which have the highest resolution for HI observations, in order to compare with the CO data of a resolution $100''$ and to examine thevertical (latitude) variation of gas density. Table 1 shows the observational parameters of the data, and Figure 1 shows examples of the HI and CO $b-v$ diagrams superposed on each other.

– Table 1, Figure 1 –

2.2 Molecular fraction

We adopt the following relations between the column density N of the atomic and molecular hydrogen and the intensity I of the HI and CO line emissions:

$$N_{\rm H}\,[\,{\rm cm}^{-2}] = C_1 I_{\rm HI} \tag{1}$$

and

$$N_{\rm H_2}\,[\,{\rm cm}^{-2}] = C_2 I_{\rm CO}\,, \tag{2}$$

where C_1 and C_2 are the conversion factors. In this paper we regard C as a constant and adopt

$$C_1 = 1.8 \times 10^{18}\ \ {\rm cm}^{-2}/({\rm K\,km\,s}^{-1}) \tag{3}$$

and

$$C_2 = 2.8 \times 10^{20}\ \ {\rm cm}^{-2}/({\rm K\,km\,s}^{-1}) \tag{4}$$

(Burton 1988; Bloemen *et al.* 1985). However, Arimoto *et al.* (1996) point out that the CO-to-H_2 conversion factor in spiral galaxies is dependent on the radial distance from the Galactic Centeras

$$C_2 = C_2^0\ 10^{0.39\,R/R_e}, \tag{5}$$

where the coefficients have been given as $C_2^0 = 0.9 \times 10^{20}\ \ {\rm cm}^{-2}/({\rm K\,km\,s}^{-1})$ and $R_e = 6.6$ kpc. Although our study will be based on an assumption of a constant C_2 factor as equation (4), we examine the effect of the radial variation of C_2 on our result, and discuss it in the last section.

The number density n is given by

$$n = N/\Delta r, \tag{6}$$

where Δr is the depth along the line of sight.

We define the molecular fraction $f_{\rm mol}$ as the ratio of the molecular hydrogen gas density to the total hydrogen gas density, which is expressed by mass density ρ or number density n by

$$f_{\rm mol} = \frac{\rho_{\rm H_2}}{\rho_{\rm H} + \rho_{\rm H_2}} = \frac{2\,n_{\rm H_2}}{n_{\rm H} + 2\,n_{\rm H_2}}. \tag{7}$$

2.3 Tangent points and Terminal-velocity method

Assuming a circularly symmetric model of the Galaxy, we can obtain distances to the emission at terminal velocities in the first and fourth quadrants ($0° < l < 90°$ and $270° < l < 360°$). The radial velocity at each galactic longitude l in the first quadrant is given by

$$v_r = \left[\frac{R_0}{R}V(R) - V_0\right]\sin l, \tag{8}$$

where $V(R)$ is the rotation velocity at galactocentric distance R, $R_0(= 8.5$ kpc) is the distance of the sun from the galactic center, and $V_0(= 220\,\mathrm{km\,s^{-1}})$ is the rotation velocity at $R = R_0$.

Terminal-velocity emission comes from the tangent point at a galactocentric radius

$$R = R_0\,|\sin l\,|, \tag{9}$$

and the galactic latitude b corresponds to the height from the galactic plane as

$$z = R_0\,\cos l\,\tan b. \tag{10}$$

The actual velocity profiles do not have a sharp cutoff due to the velocity dispersion of the gas. So, we regard the integrated emission within a certain velocity range of width Δv around the terminal velocity as a contribution of the gas at the tangent point. We adopt a velocity width $\Delta v = 6.5\,\mathrm{km\,s^{-1}}$ at any longitude, which we found to be a typical width of the CO velocity profile corresponding to a terminal-velocity emission component at $b \simeq 0$. In fact, this value is consistent with the velocity dispersion obtained by Malhotra (1994), who finds that the value of the velocity dispersion varies $3.8\,\mathrm{km\,s^{-1}}$ at 2.5 kpc to 7.1 $\mathrm{km\,s^{-1}}$ at 7.5 kpc. The depth along the line of sight corresponding to this velocity width is given by

$$\begin{aligned}\Delta r &= 2R_0\,\sin l\,\left[\left(\frac{V_0}{V_0 - \Delta v}\right)^2 - 1\right]^{1/2} \\ &\approx 0.50\,R_0\,\sin l.\end{aligned} \tag{11}$$

Based on these relations we calculated number densities of H and H_2 at each longitude and latitude using latitude-velocity $(b - v)$ diagrams, and obtained vertical density distributions as a function of height z from the galactic plane. Then, we arranged the thus obtained z distributions at various longitudes in the order of the distance from the galactic center, and obtained two dimensional maps of the distributions of H and H_2 gases in the (R, z) plane.

3 Result

3.1 HI and H_2 Distributions

As seen from the $b - v$ diagram (Figure 1), the HI gas is distributed smoothly in the velocity direction at any longitude, and therefore, at any point along the line of sight.

On the other hand, the H_2 gas distribution is clumpy. The HI and H_2 distributions in the z direction are also clearly different (Figure 2): the HI distribution has a flat plateau near the galactic plane and gentle skirts, while most of H_2 profiles have multiple peaks, and the maximum density is much higher than that of HI. The CO distribution is not centered on the Galactic plane, which is consistent with previous studies (Malhotra 1994; Dame *et al.* 1987).

– Figure 2 –

Figures 3*a* and *b* show the (R, z) distributions of HI and H_2, respectively. These figures, therefore, represent cross sections of our Galaxy along the tangent velocity circle. The density distribution of HI gas in the z direction extends for a few hundred parsecs, while the extent of H_2 is not more than 100 pc: there is little CO emission at high latitudes. Note, however, that these two cross sections are not fully sampled in the longitude direction, because the observations have been obtained every $\Delta \sin l = 1/40$ ($\Delta l = 1.^\circ 4 \,/\, \cos l$: $\Delta R = 212.5$ pc) with a beam width $4'$ for HI and $100''$ for CO.

– Figure 3 –

In Figure 4, we show an (R, z) distribution of H_2 gas for the whole range covered by the present CO data from the galactic center region ($l = 10^\circ, R = 1.49$ kpc) to the solar neighborhood ($l = 77^\circ, R = 8.29$ kpc). This figure includes the region shown in Figure 3*b*. Figure 5(a) shows radial distributions of HI and H_2 gases averaged at $|z| < 100$pc. A radial distribution of CO emissivity in our Galaxy has been obtained by Robinson *et al.* (1988) and Sanders *et al.* (1984). Our result is approximately agree with theirs. The variation of the H_2 number density is much larger than that of HI. Note that the highest density region for H_2 in Figure 4 and 5 corresponds to the '4-kpc molecular ring', and that the H_2 gas density in the inner region within 3 kpc and outside of 7 kpc is an order of magnitude smaller than that in the 4-kpc ring. Figure 5(b) shows the same as Figure 5(a) but using the C_2 factor as given by equation (5), which takesinto account the radial variation of the CO-to-H_2 conversion factor. The H_2 density distribution changes drastically in the inner region of the Galaxy, indicating much less molecular gas within $R \sim 4$ kpc.

– Figure 4, 5 –

3.2 Variation of $f_{\rm mol}$

We calculated $f_{\rm mol}$ for a region shown in Figure 3, where both the HI and H_2 densities are obtained. Negative values in the observed CO intensity (H_2 density) have been replaced with zero. Figure 6 shows an example of the z-variation of $f_{\rm mol}$ at $l = 53^\circ$. It is evident that the value of $f_{\rm mol}$ is almost unity near the galactic plane, and decreases rapidly to zero in a narrow range of z as z increases.

This phenomenon is commonly seen at all longitudes except at $l = 61°$ and $64°$ ($R \leq 7.5$ kpc) where the amount of H_2 is small. This fact indicates the existence of a z-directional boundary of a region with a high H_2 fraction, which we call the molecular front in the z-direction. Most of hydrogen gas is in the molecular phase in the region near the galactic plane, sandwiched between the two molecular fronts, whereas in the outer (higher) region it is in the atomic phase.

– Figure 6 –

Figure 7 shows the two dimensional distribution of $f_{\rm mol}$ as a contour map in the (R, z) plane. The centroid of the molecular dominant disk, where $f_{\rm mol} \geq 0.8$, is waving, corresponding to the fact that the molecular gas disk is corrugating (e.g. Malhotra 1994). It is remarkable that the thickness of the molecular dominant disk is almost constant at 109 ± 12 pc. On the other hand, it is known that the scale height of the HI layer is larger than it. A thickness of HI layer between half-density points has approximately constant value: 220 kpc over $4 \leq R \leq 8$ kpc (Dickey and Lockman 1990). When we compare the thickness of molecular dominant disk with the scale height of HI gas, we can express that the atomic hydrogen layer wraps the molecular disk.

– Figure 7 –

Figure 8(a) shows radial variations of the molecular fraction calculated for number densities of HI and H_2 averaged within $|z| < 50$ and 200 pc of the galactic plane. In both cases the molecular fraction decreases from 0.8 to 0.6 with increasing R. Though we can not clearly see the phase transition in this region, curves are consistent with the fact that the molecular fraction is almost unity in the the central few kpc region (Sofue *et al.* 1994). Particularly, the curve for $|z| < 200$ pc indicates a decrease of $f_{\rm mol}$ beyond $R \simeq 7.5$ kpc. This may be consistent with the existence of the radial molecular front indicated from an analysis of longitude-velocity diagrams of the Galaxy (Sofue *et al.* 1994). Since the H_2 gas density over $R \geq 8$ kpc is much smaller than that of inner region (Dame *et al.* 1987), it is expected that the molecular fraction will decrease suddenly beyond this radius. Figure 8(b) shows the same variation but considering the radial dependency of CO-to-H_2 conversion factor. The radial molecular front slightly change. However, no significant effect is found.

– Figure 8 –

3.3 Model Analysis

The three crucial parameters which determine $f_{\rm mol}$ are the interstellar pressure (P), the intensity of dissociative UV radiation field (U), and the metal abundance (Z) which is related to the amount of interstellar dust and shields UV photon (Elmegreen 1993). Based on the phase-transition theory (Elmegreen 1993), Honma *et al.* (1995) has developed a

computing code to model the molecular front in galactic scale. By applying this code, we calculate the variation of molecular fraction in the z-direction.

Since it is reasonable to assume that the pressure is proportional to the gas density, we consider the following two cases: first, $P(z)$ is traced by the observed total gas density distribution in the z-direction ($n_{\rm tot}$), and second, $P(z)$ is expressed by a gaussian function of z, considering the hydrostatic balance of the gas pressure with the gravity in the z-direction. According to van der Kruit and Searle (1982) we assume that the intensity of the radiation field is expressed as

$$U(R,z) = U_0\, e^{(-R/R_{\rm U})}{\rm sech}^2(z/z_0), \tag{12}$$

where $R_{\rm U} = 5.0$ kpc is a scale distance from the galactic center, and $z_0 = 0.7$ kpc is the scale height in the z-direction. For the metallicity, we do not have any information about the gradient in the z-direction. So, we assume that the value of Z is constant against z, while it varies with R as $Z = Z_0\, e^{-(R-R_0)/R_Z}$.

– Figure 9 –

Figure 9 shows a thus calculated variation of the molecular fraction for $l = 53°$. The solid line corresponds to the observed $n_{\rm tot}(z)$, and the dashed line to the gaussian distribution of $P(z)$ in which the parameter of the gaussian function was taken so that it fits the observed $n_{\rm tot}(z)$. Even for such a round pressure distribution as a gaussian, $f_{\rm mol}$ shows a shoulder-like variation, indicating the phase transition clearly. The curve of $f_{\rm mol}$ calculated for the observed $n_{\rm tot}(z)$ shows a sharper variation at a critical height, and agrees well with the observed $f_{\rm mol}$ variation (Figure 6) and reproduces the molecular front in the z-direction. Though it has been considered that the most important parameter for the molecular front is the metal gradient (Honma *et al.* 1995), our results shows that the molecular front is reproduced without a metal gradient.

4 Discussion

The radial molecular front has been observed in our Galaxy as well as in many external galaxies (Sofue *et al.* 1994; Honma *et al.* 1995), in which the front is found at $R \sim 5 - 10$ kpc. In our result for our Galaxy, although $f_{\rm mol}$ is almost unity in $4.8 \leq R \leq 7.2$ kpc, the radial decrease of $f_{\rm mol}$ may occur at $R \geq 7.5$ kpc, where the value of $f_{\rm mol}$ drops from ~ 0.8 to less than 0.6. Since the HI gas density varies more gradually than the H_2 gas at $R \geq 7$ kpc, we may expect that the molecular gas is not any more dominant in the outer region of $R = 7.5$ kpc. This indicates that the molecular front in our Galaxy is located at $R \simeq 7.5$ kpc and the transition region from H_2 to HI and vice versa is as narrow as $\Delta R \sim 2$ kpc in the radial direction.

From the z-directional variation of $f_{\rm mol}$, we found the molecular fronts in the direction perpendicular to the galactic plane. The molecular hydrogen disk is sandwiched by a

thicker HI envelope. In the molecular region near the galactic plane, between the two fronts, the ISM is almost totally in the molecular phase with $f_{\rm mol} \geq 0.8$, while in the outer region, the gas is almost totally HI. We stress that the transition between HI and H_2 is taking place within the narrow range at a height of $z \simeq \pm 50$ pc at $R \leq 7$ kpc.

In this paper, we have not taken to account a metallicity gradient in the z-direction, since the existence of the z-gradient of the metallicity has not been reported. Even if it exists, the scale height of the variation would be a few hundred pc, because it will reflect the scale height of old population stars. Therefore, it will be reasonable to assume that the metallicity gradient in z-direction is small or not present in our region of $|z| < 100$ pc.

It has been found that the CO-to-H_2 conversion factor (C_2 factor) increases exponentially with the radius due to the metallicity gradient (Arimoto *et al.* 1996). This implies that the C_2 value in the region considered here (from R=4 to 7 kpc) varies by a factor of 1.5. We have examined the radial variations of the H_2 density and $f_{\rm mol}$ by taking into account this effect. We found that the radial molecular front slightly moves outwards, but not significant change of the property of the $f_{\rm mol}$ distribution in the z-direction was found.

We thank M. Honma for his valuable comments and for providing us with the code to model the molecular front. We are also indebted to Drs. T. M. Bania, G. R. Knapp, and S. Malhotra for providing us with the HI and CO data in a machine readable formats.

References

Arimoto N., Sofue Y., and Tsujimoto T., 1996, PASJ Vol 48 in press.

Bania, T. M., and Lockman, F. J., 1984, ApJS 54, 513.

Bloemen, J.B.G.M., Strong, A. W., Cohen, R. S., Dame, T. M., Grabelsky, D. A., Hermsen, W., Lebrun, F., Mayer-Hasselwander, H. A., and Thaddeus, P., 1985, A&A 154, 25.

Burton, W. B., and Gordon, M. A., 1978, A&A 63, 7.

Burton, W.B. 1988 in Galactic and Extragalactic Radio Astronomy, edited by G. L. Verschuur and K. I. Kellermann (Springer-Verlag, Berlin), Chap. 7.

Combes F., 1992, ARA&A 29, 195.

Dame, T. M., Ungerechts, H., Cohen, R. S., de Geus, E. J., Grenier, I. A., May, J., Murphy, D. C., Nyman, L. -A., and Thaddeus, P., 1987, ApJ 322, 706.

Elmegreen, B. G., 1993, ApJ 411, 170.

Honma, M., Sofue, Y., and Arimoto, N., 1995, A&A 304, 1.

Knapp, G. R., Stark, A. A., and Wilson, R. W., 1985, AJ 90, 254.

Lockman, F. J., 1984, ApJ 283, 90.

Malhotra, S., 1994, ApJ 433, 687.

Sanders, D. B., Solomon, P. M., and Scouville, N. Z., 1984, ApJ 276, 182.

Sofue, Y., Honma, M., and Arimoto, N., 1995, A&A 296,33. ApJ 319, 730

van der Kruit, P.C., and Searle, L., 1982, A&A 110, 61.

Figure captions

Figure 1. A latitude-velocity ($b - v$) contour map of the HI brightness temperature at $l = 39°$. The ordinate is galactic latitude in degrees, and the abscissa is velocity relative to the LSR in km s^{-1}. Contours are drawn at 10% interval of the peak brightness (114 K). A $b-v$ map of the CO emission at $l = 39°$ is superposed in gray scale.

Figure 2. Vertical distributions of the atomic hydrogen gas (doted line) and the molecular hydrogen gas (solid line) at $l = 53°$. The ordinate is the number density in HI cm^{-3} and H_2 cm^{-3}. (Note that the ordinate scaling for H_2 should be doubled when comparing the two curves in mass.) The abscissa is the height from the galactic plane.

Figure 3. (*a*) The (R, z) distribution of the HI gas density. Contours are drawn at intervals of 0.01 H cm^{-3}. (*b*) The (R, z) distribution of the H_2 gas density. Contours are drawn at intervals of 0.1 H_2 cm^{-3}.

Figure 4. The (R, z) distribution of the H_2 gas density for the whole range of the CO data. Contours are drawn at intervals of 0.2 H_2 cm^{-3}.

Figure 5. (*a*)Radial distributions of HI gas density (doted line) and H_2 gas density (solid line) averaged in $|z| < 100$ pc. (*b*) The same, but including the radial variation of the CO-to-H_2 conversion factor C_2 as given by equation (5).

Figure 6. The molecular fraction at $l = 53°$ as a function of z. The ordinate is $f_{\rm mol}$.

Figure 7. The (R, z) distribution of the molecular fraction. Contours are drawn at an interval of 0.2. Dashed lines show $f_{\rm mol}$= 0.2, 0.4, and solid lines $f_{\rm mol}$= 0.6, 0.8.

Figure 8. (*a*) Radial variations of the molecular fraction averaged within $|z| < 50$ pc (solid line) and 200 pc (dashed line). (*b*) The same as (*a*) but including the effect of radial dependency of CO-to-H_2 conversion factor.

Figure 9. The molecular fraction calculated theoretically for $l = 53°$. The solid line is for the case where the observed $n_{\rm tot}(z)$ was used to calculate $P(z)$. The dashed line corresponds to a gaussian distribution of $P(z)$. The doted line shows the observed $f_{\rm mol}$ (Fig. 6).

Table 1. Observational parameters

	HI	CO ($J = 1 \rightarrow 0$)
	Bania and Lockman (1984)	Knapp *et al.* (1985)
Telescope	Arecibo	Bell Laboratories
Aperture	304 m	7 m
Wavelength	21 cm	2.6 mm
HPBW	$4'$	$1'40''$
Longitude extent	$33^\circ \sim 64^\circ$	$10^\circ \sim 77^\circ$
Latitude extent	$\pm 3^\circ$	$\simeq \pm 2^\circ$
Δv	$1.03\ \mathrm{km\,s^{-1}}$	$0.65\ \mathrm{km\,s^{-1}}$
Δb	$2'$	$2'$
R (kpc)*	$4.68 \sim 7.65$	$1.49 \sim 8.29$
Longitude interval	$\Delta \sin l = 0.025$, or $\Delta l = 1^\circ.43/\cos l$	
Radius interval	$\Delta R = R_0 \Delta \sin l = 212.5$ pc	

* The distance to the Galactic Center is taken to be $R_0 = 8.5$ kpc.

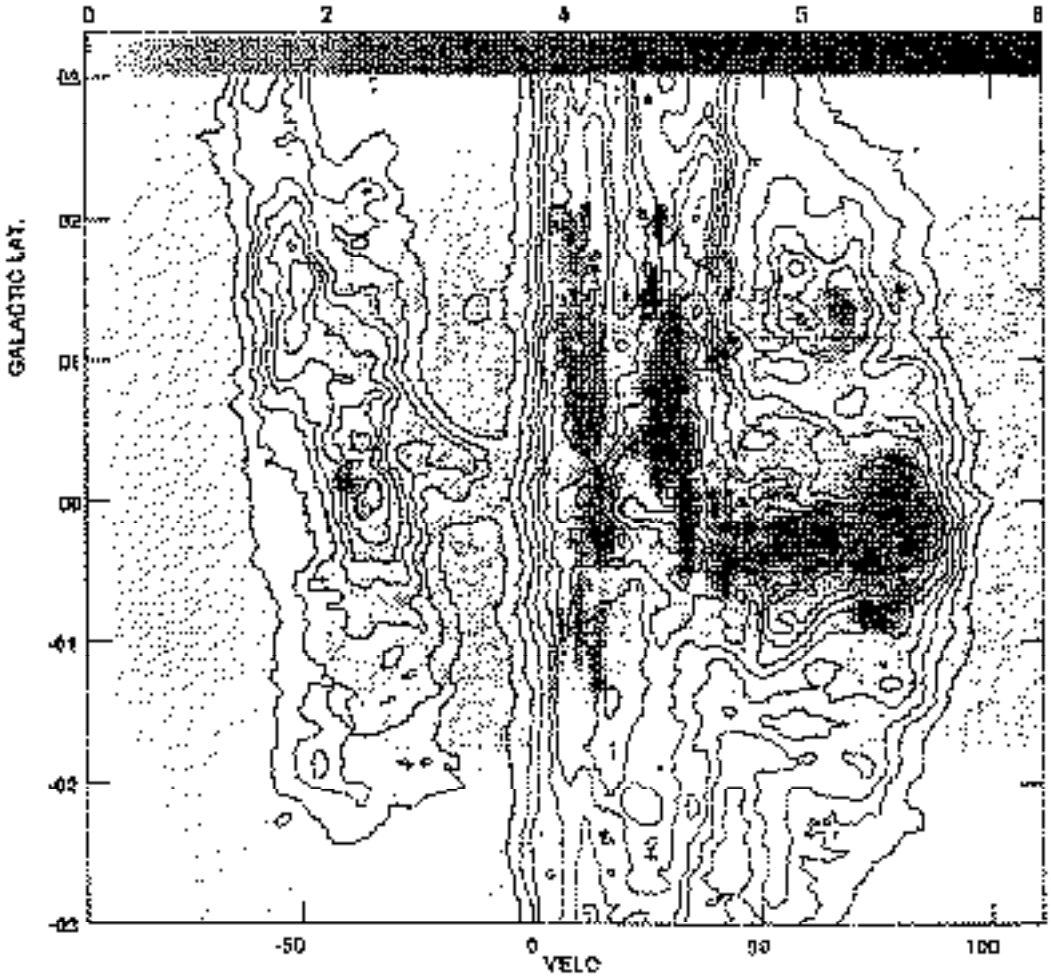

Fig. 1

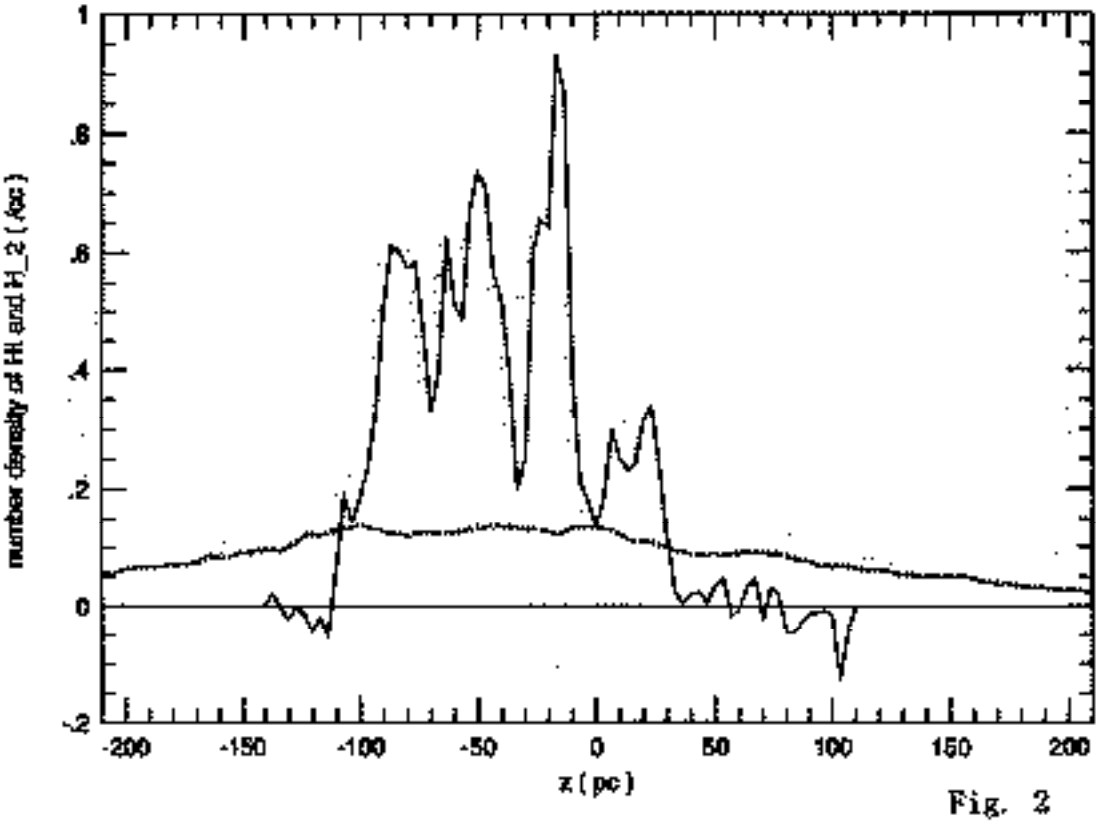
number density of HI and H_2 (/cc)
1
.8
.6
.4
.2
0
-.2
-200
-150
-100
-50
0
50
100
150
200
z (pc)

Fig. 2

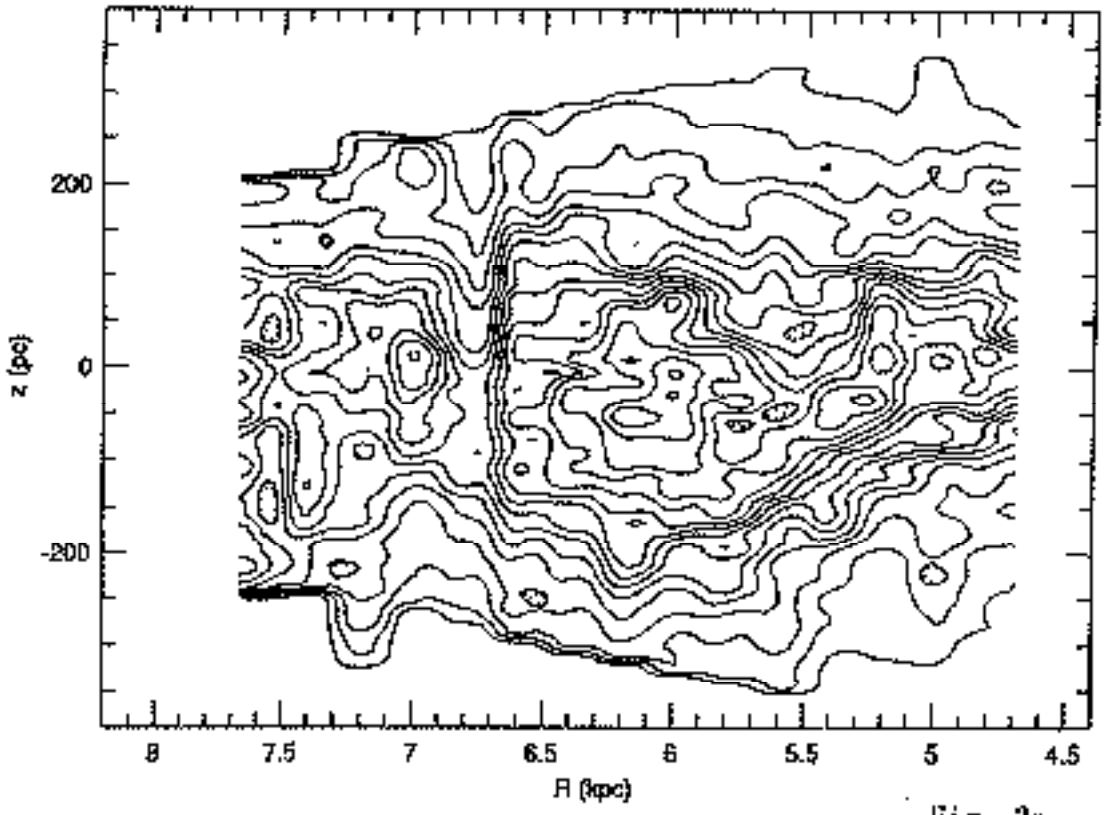
200
0
-200
z (pc)
8
7.5
7
6.5
6
5.5
5
4.5
R (kpc)

Fig. 3a

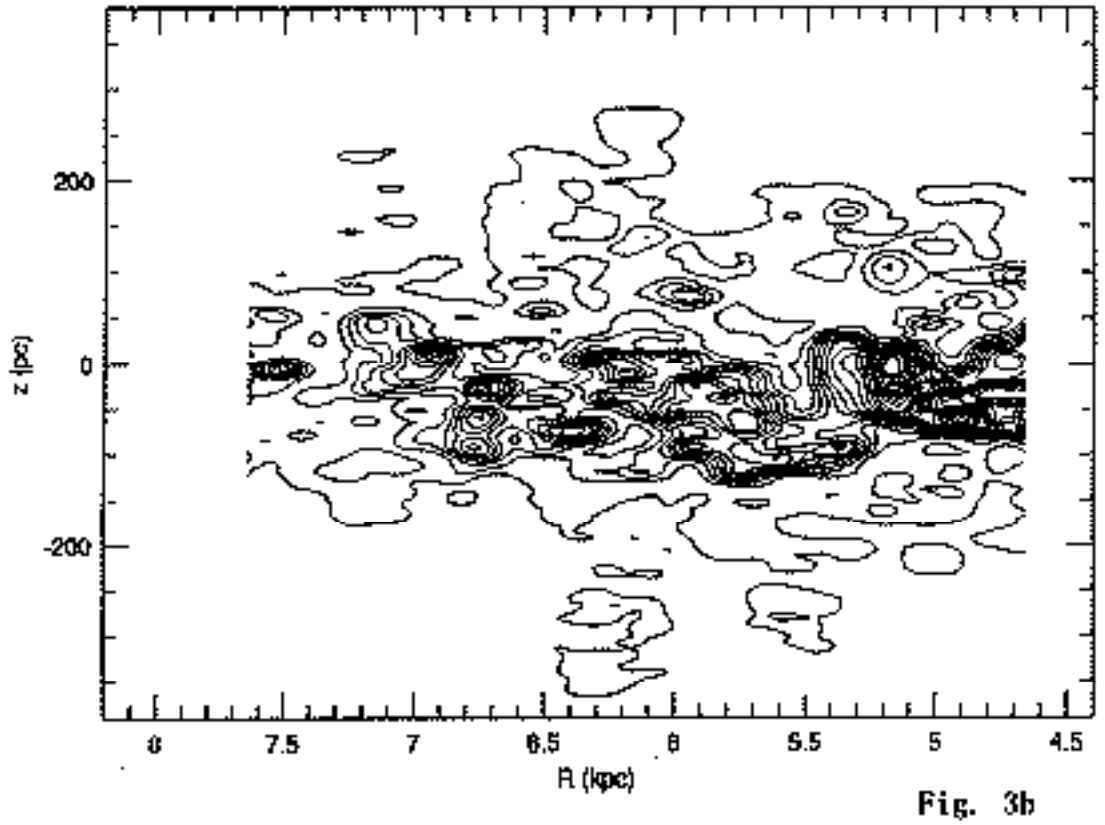
200
0
-200
z (pc)
8
7.5
7
6.5
6
5.5
5
4.5
R (kpc)

Fig. 3b

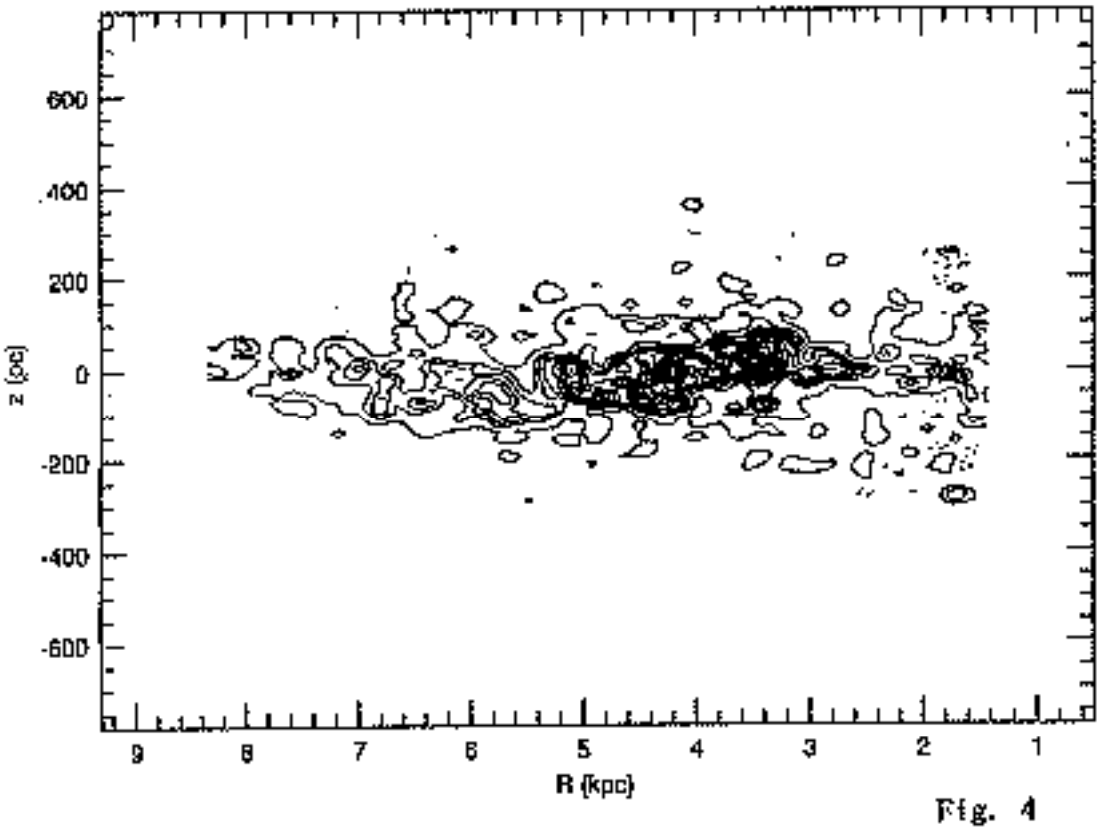

Fig. 4

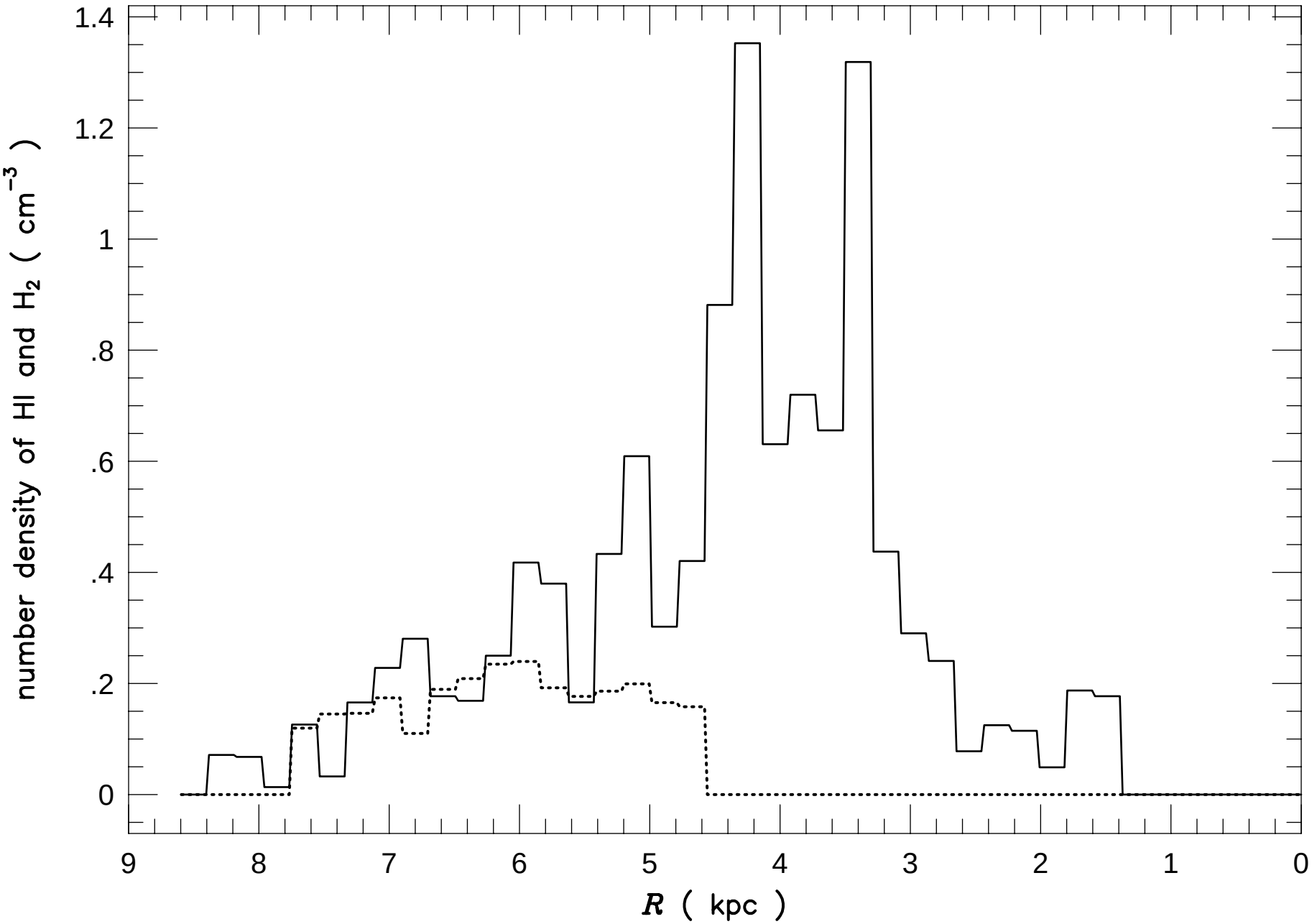
1.4
1.2
1
.8
.6
.4
.2
0
number density of HI and H_2 (cm^{-3})
9
8
7
6
5
4
3
2
1
0
R (kpc)

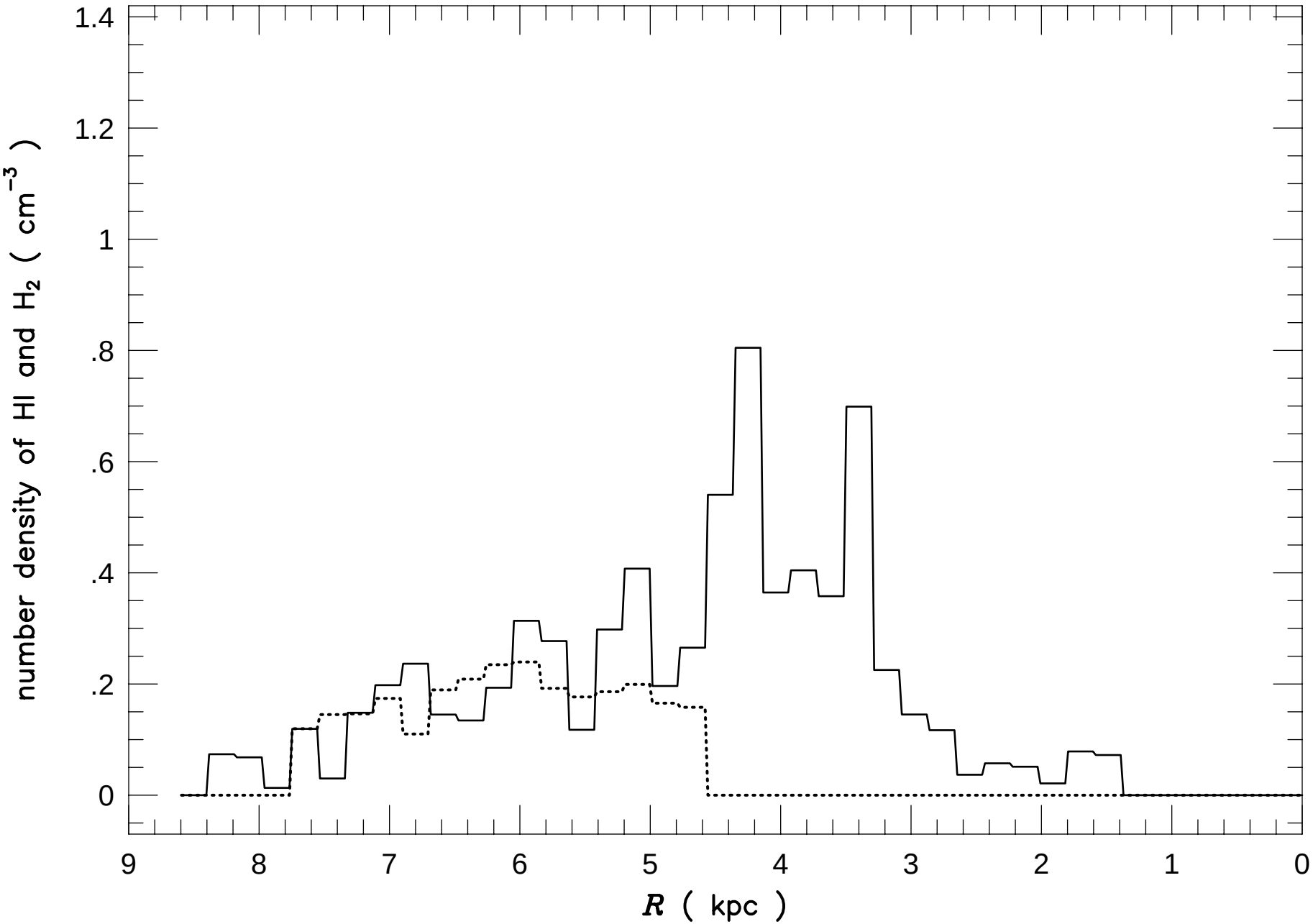
1.4
1.2
1
.8
.6
.4
.2
0
number density of HI and H_2 (cm^{-3})
9
8
7
6
5
4
3
2
1
0
R (kpc)

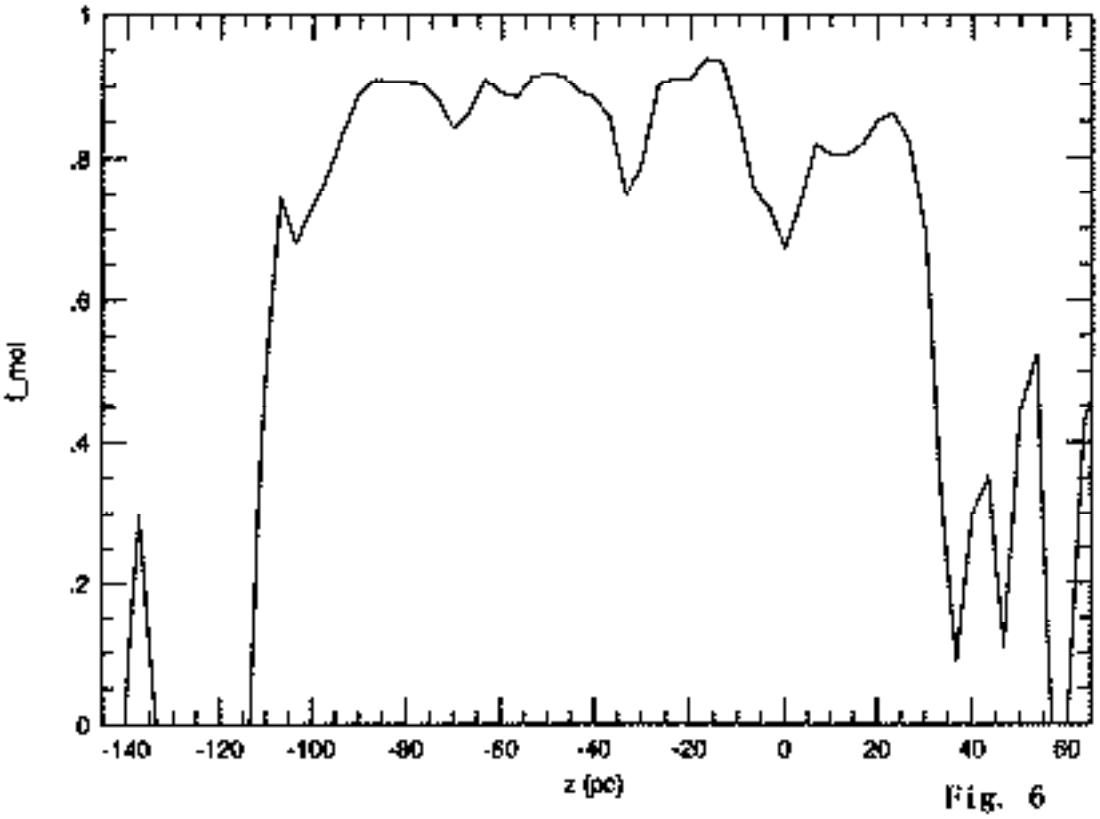

Fig. 6

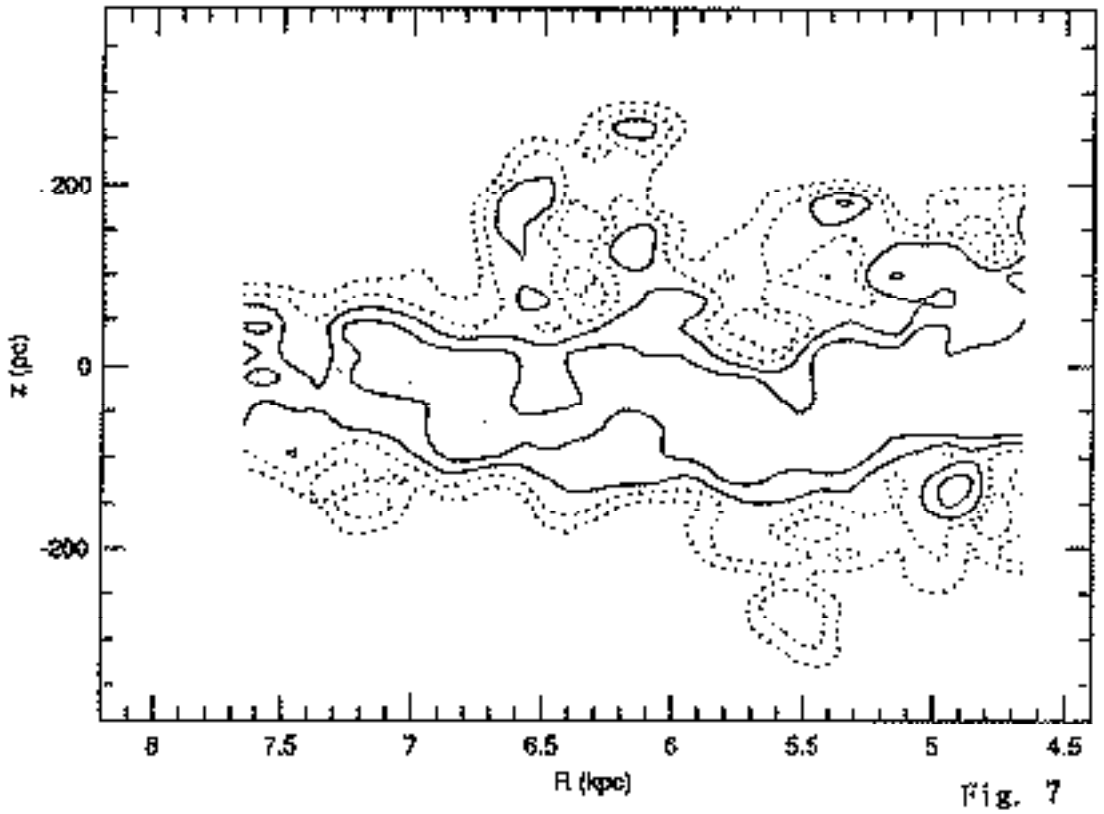

Fig. 7

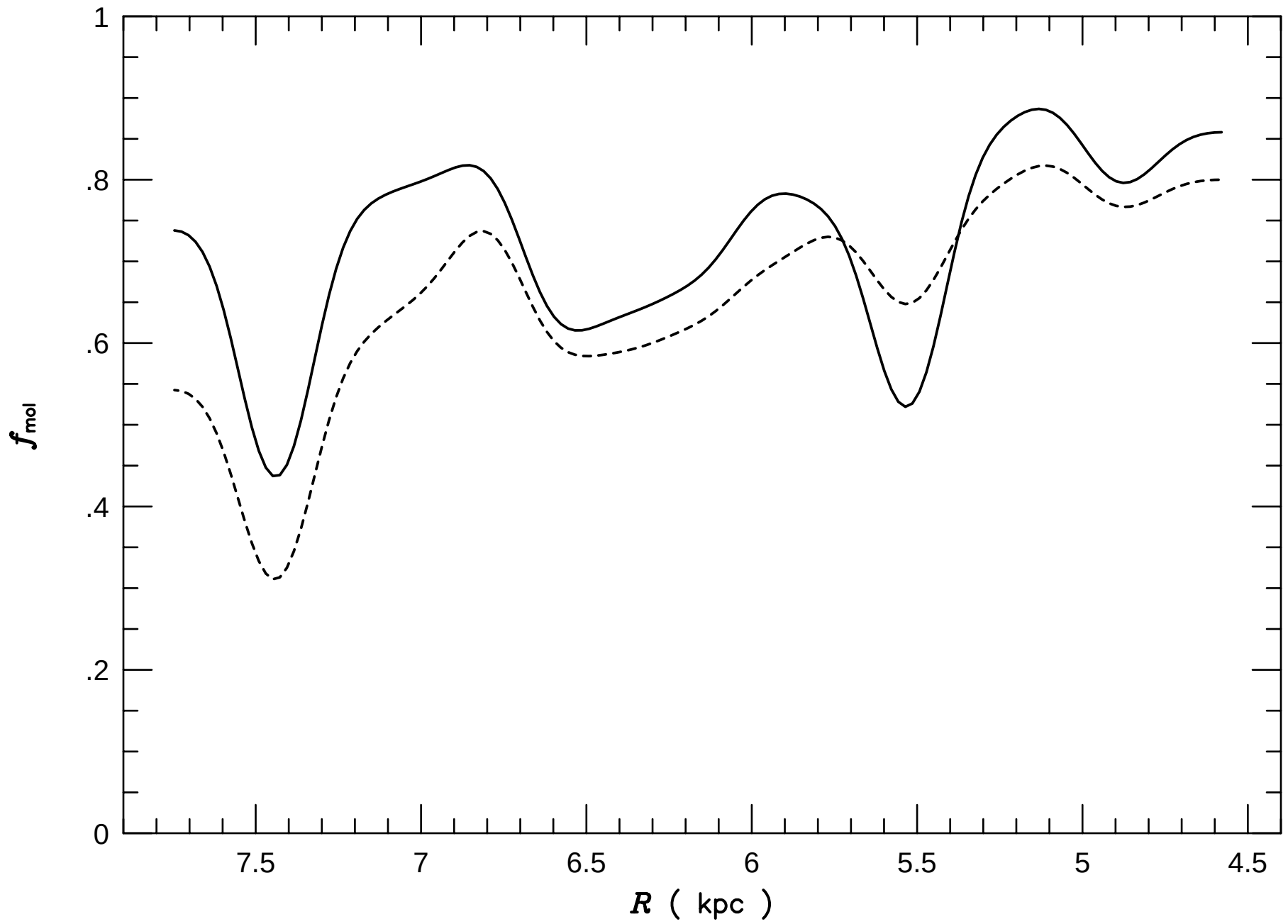
1
.8
.6
.4
.2
0
f_{mol}
7.5
7
6.5
6
5.5
5
4.5
R (kpc)

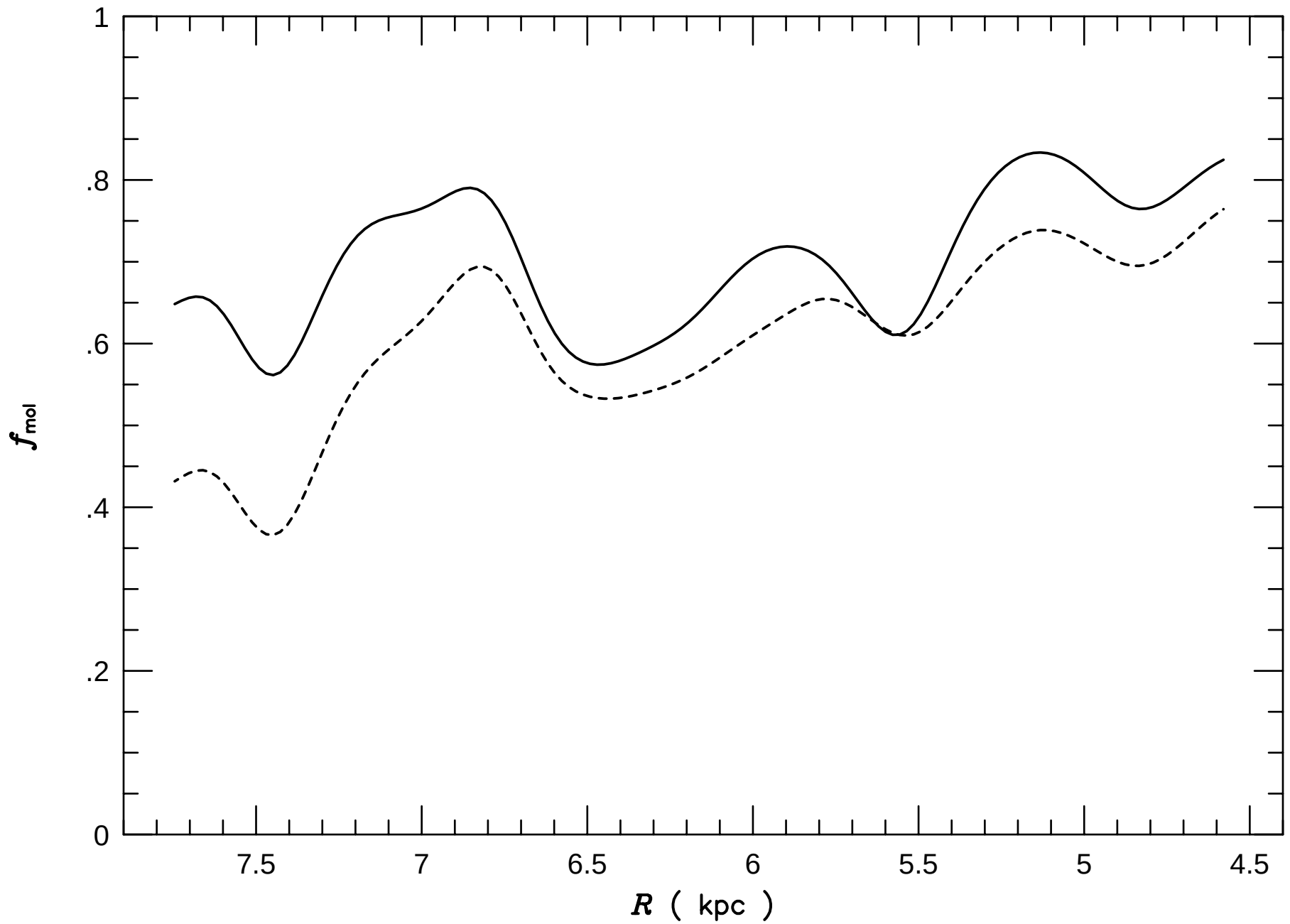
1
.8
.6
.4
.2
0
f_{mol}
7.5
7
6.5
6
5.5
5
4.5
R (kpc)

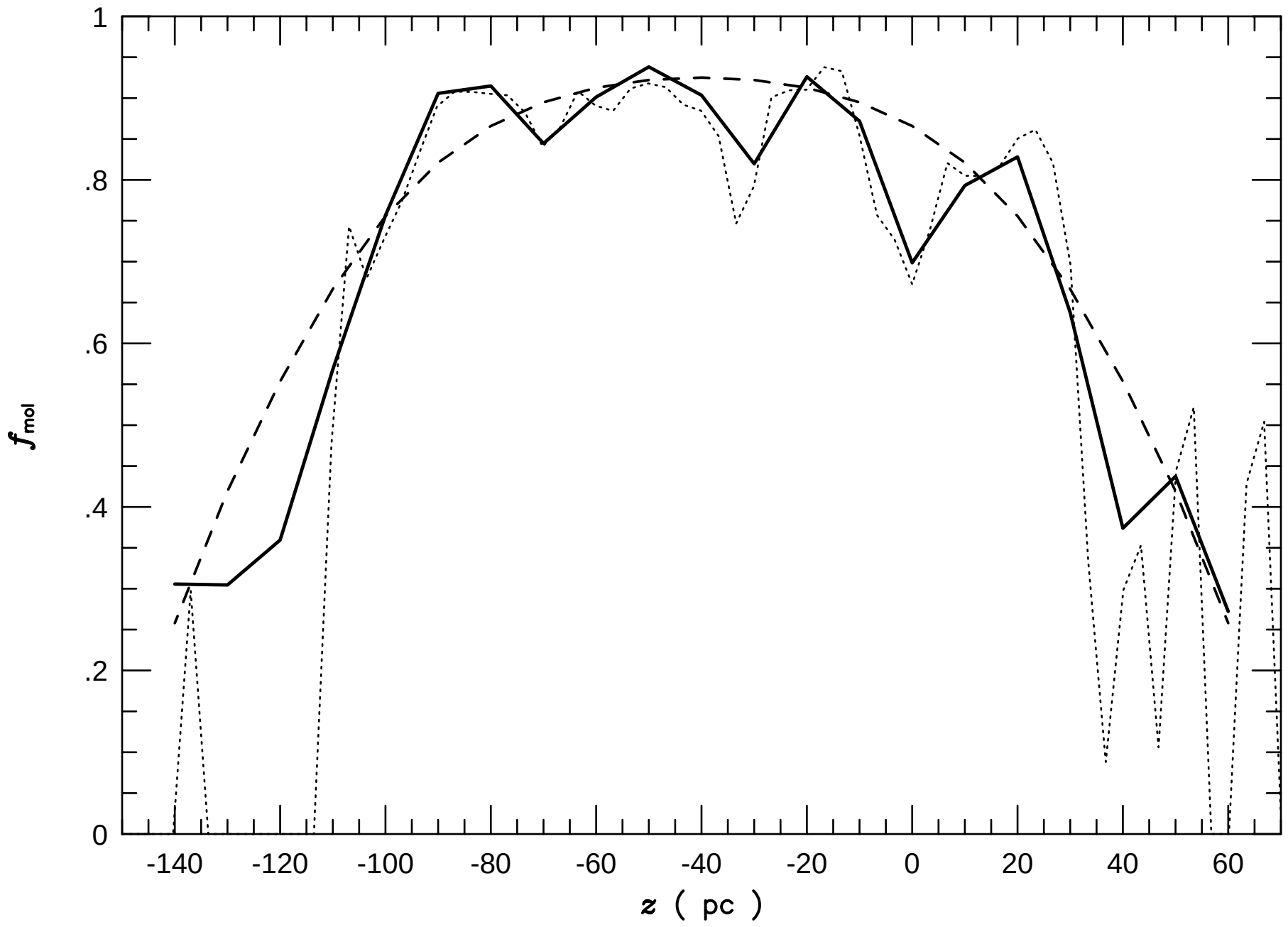
1
.8
.6
.4
.2
0
f_{mol}
-140
-120
-100
-80
-60
-40
-20
0
20
40
60
z (pc)